P13.8 Recognition of lightning echoes with the polarimetric WSR-88D

Valery Melnikov, Terry Schuur, and Alexander Ryzhkov

Cooperative Institute for Mesoscale Meteorological Studies, Oklahoma University and NOAA/OAR National Severe Storms Laboratory, Norman OK.

1. Introduction

Within the next year, the US National Weather Service will begin to upgrade the national network of WSR-88D weather radars to include polarimetric capabilities (e.g., Istok et al. 2009). **S**imultaneous transmission and reception of **H**orizontally and **V**ertically polarized waves (SHV mode) was chosen for this upgrade and implemented on the prototype polarimetric WSR-88D (hereafter referred to as KOUN), located in Norman, OK (Doviak et al. 2000). The concept of polarimetric measurements in SHV mode was tested on KOUN during the JPOLE experiment (Schuur et al, 2003).

One of the primary advantages of polarimetric radars is their ability to classify hydrometeors types (rain, snow, hail), as well as to identify non-meteorological echoes resulting from birds, insects, and ground (Zrnic and Ryzhkov 1999, Liu and Chandrasekar 2000, Zrnic et al. 2001, Schuur et al. 2003). Automated fuzzy logic Hydrometeor Classification Algorithms (HCAs), which are based on measurements in a single radar resolution volume and the spatial characteristics of some parameters along the radar radial, are then used to delineate weather echoes from non-meteorological returns.

After analyzing KOUN's data collected in thunderstorms, we have noticed that the weather echoes are sometimes disrupted by non-meteorological returns caused by lightning. All radar parameters experience these disruptions which, in turn, also affects the HCA results. To eliminate misclassifications by the HCA, it is necessary to better understand the variations of radar variables caused by lightning. In this paper we document these variations.

SHV mode will be the primary operational mode for the WSR-88D but the radar hardware will also be capable of conducting depolarization measurements. In this mode, the full energy is injected at horizontal polarization and both horizontally and vertically polarized returns are received. This mode will be referred to as LDR mode because the main polarimetric measurable is the Linear Depolarization Ratio. Cross-polarization properties of lightning echoes have been studied at L and X-bands by Mazur and Walker (1982), Krehbiel et al. 1991, and Caylor et al. (1993). To our knowledge, there have been no reports on cross-polarization properties of lightning echoes at S-band. In this paper, we document disturbances to the radar variables during lightning for LDR mode.

Valery.Melnikov@noaa.gov

2. Types of disruptions

Radar observations with KOUN show that there are two types of "non-meteorological" disruptions to weather echoes caused by lightning. Examples are provided by the RHI vertical radar cross sections shown in Fig. 1. The first type (Fig. 1b) appears in the form of "outlier" echoes; note a significant drop in the copolar correlation coefficient at distances of 80 to 95 km and at heights of 5 to 6 km. The disruption is more than 10 km long with a duration of 500 ms, i.e, several radar dwell times. Because of the low correlation coefficient, this disruption can be confused with the presence of hail. This type of disruption is caused by echoes from lightning (Caylor et al. 1993, Caylor and Chandrasekar 1996).

The second type of disruption appears in the form of "outlier" radials; in Fig. 1c, one can see three such radials at elevations of 0.8^o, 7.3^o, and 11.4^o. These "outliers" are caused by wideband lightning radiation intercepted by the antenna. Lightning radiation significantly increases noise and can be received through the antenna sidelobes, so it is possible that there may be no lightning echoes the in disrupted radials. This type of disruption is caused by wideband noise-like lightning radiation and can be eliminated by utilizing the 1-lag estimators, which are immune to noise (Melnikov and Zrnic, 2006). The field of 1-lag estimators of the correlation coefficient is shown in Fig. 1d. The 1-lag estimators eliminate such disruptions in the differential reflectivity fields as well (not shown). Because it is possible to eliminate the second type of disruption, we hereafter focus on the first type, i.e., on radar echoes from lightning.

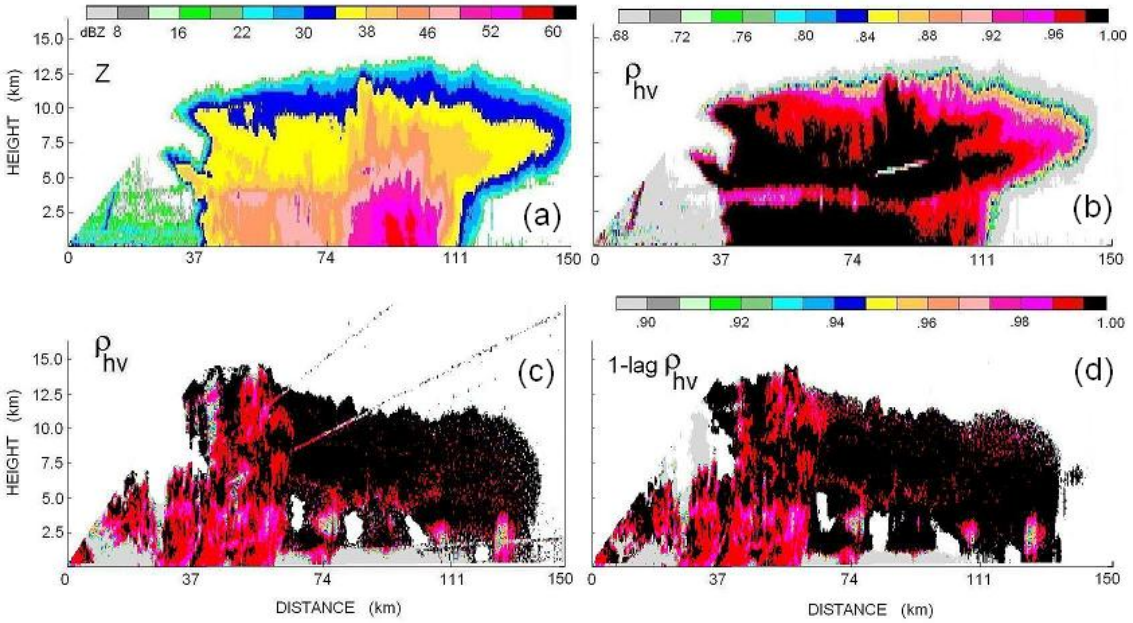

Fig. 1. RHIs collected in SHV mode on (a,b) 1 July, 2005 at 1258 in azimuth of 120°, (c, d) on 17 August, 2006 at 1155.

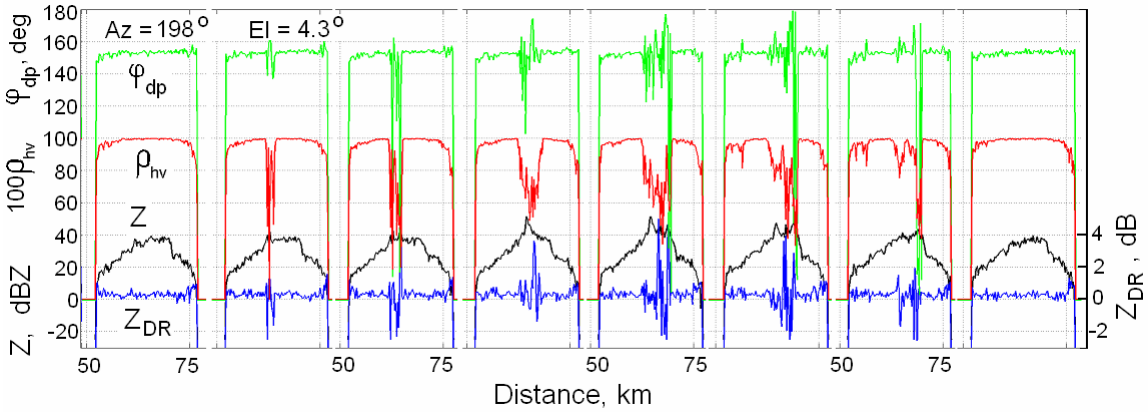

Fig. 2. Consecutive range profiles of Z, Z_{DR}, φ_{dp}, and ρ_{hv} on July 22, 2006 at 0016:24. M =128, PRF = 1013 Hz. Range numbers are shown in each other panels.

Radar echoes from lightning are rare events but it is nevertheless necessary that the HCA has the ability to recognize and eliminate or tag them. Parameters of radar variables from lightning must therefore be studied. We know the only paper by Caylor at al. (1993) that documented the polarimetric parameters of lightning echo at S-band in Florida. We present our results obtained in central Oklahoma. Because lightning can change spectral characteristics of radar returns (Zrnic et al. 1982, Mazur et al. 1987), we also study properties of the Doppler velocity and spectrum width.

To shorten the update time of radar observations, phased array radars, PAR, at X- and S-bands are used (e.g., Heinselman et al 2007, Blustein et al, 2007). Utilization of polarimetric weather PARs are under consideration. Often PAR estimate radar parameters with smaller number of pulses. We show data of polarimetric properties of lightning at small number of samples that can be utilized with conventional polarimetric radar and PARs.

3. Parameters of lightning echoes in SHV mode

In SHV mode, six radar variables are measured in each radar resolution volume: reflectivity, Z, the Doppler velocity, V, spectrum width, σ_v , differential reflectivity, Z_{DR}, differential phase, φ_{dp}, and copolar correlation coefficient, ρ_{hv}. A detailed description of these variables can be found in Doviak and Zrnic (1993) while the main features of the SHV mode have been discussed in Doviak et al. (2000).

Radar echoes from lightning are usually observed by stationary antenna, which reduces changes in echoes due to antenna movement and provides better estimates of the radar variables in the same radar resolution volumes before and after lightning. We have analyzed KOUN data collected with both stationary and a slow moving antenna. For a moving antenna, vertical radar cross sections collected with a vertical rate of less than 0.2^o s^{-1} have been analyzed. Range profiles from before, during, and after a lightning strike are presented in Fig. 2. Reflectivity in the horizontal channel is denoted as Z, M is the number of samples, and PRF is the pulse repetition frequency. Perturbations of echo caused by lightning are seen at distances from 58 to 65 km in the six inner profiles. The height of the lightning echo is about 4.5 km. The first and last profiles have close radar parameters and represent the profiles before and after lightning. To obtain polarimetric characteristics of lightning echoes, KOUN's data with 128 and 256 samples were used. Such a large number of samples allows for an accurate estimation of radar variables both before and after lightning. Pitfalls are rather coarse estimation of the duration of lightning echoes and smoothing of their parameters.

Disturbances in the differential phase seen in Fig. 2 can lead to false calculations of the specific differential phase, $K_{\rm dp}$, and can also be confused with the presence of the phase upon backscattering δ. Disturbances in ρ_{hv} could be confused with hail signatures. $Z_{\rm DR}$ experiences large variations, both positive and negative, and Z increases by more than 10 dBZ at some ranges. Combined, these fluctuations can lead to a misclassification by the HCA and an overall reduction in data quality.

a) Radar data processing

Radar echoes of lightning have been identified by a visual inspection of consecutive radials, as in Fig. 2. A group of radials with similar radar variables in the first and last profiles and with significant deviations in Z and Z_{DR} have been selected. The following criteria have been used for the selection: at least one profile in the group has a deviation of Z exceeding 3 dB and a deviation of Z_{DR} exceeding 1 dB at least in one range gate. These are applied at SNR larger than 10 dB to eliminate noise fluctuations. If these conditions are satisfied, then neighboring range gates are examined if exceeding at least one of the above thresholds. Consecutive range gates fulfilling these criteria form a distinct lightning echo.

Caylor at al. (1993) have employed different criteria based on change of reflectivity and the correlation coefficient; the criteria used by both Caylor et a. (1993, hereafter referred to as CCBM) and this study are listed in Table 1. We employed the power criteria, i.e., the deviation of Z and Z_{DR} because of the presence of interference signals at KOUN's site. Interference signals drop ρ_{hv} by about 0.1 but did not exceed the thresholds imposed on Z and Z_{DR} by the chosen criteria.

Table 1. Criteria of lightning echo recognition with S-band polarimetric radars

Parameter	CCBM	This study
SNR, dB	30	10
Z deviation, dB	2	3
ρ_{hv} drop	0.075	N/A
Z_{DR} absolute deviation, dB	N/A	1

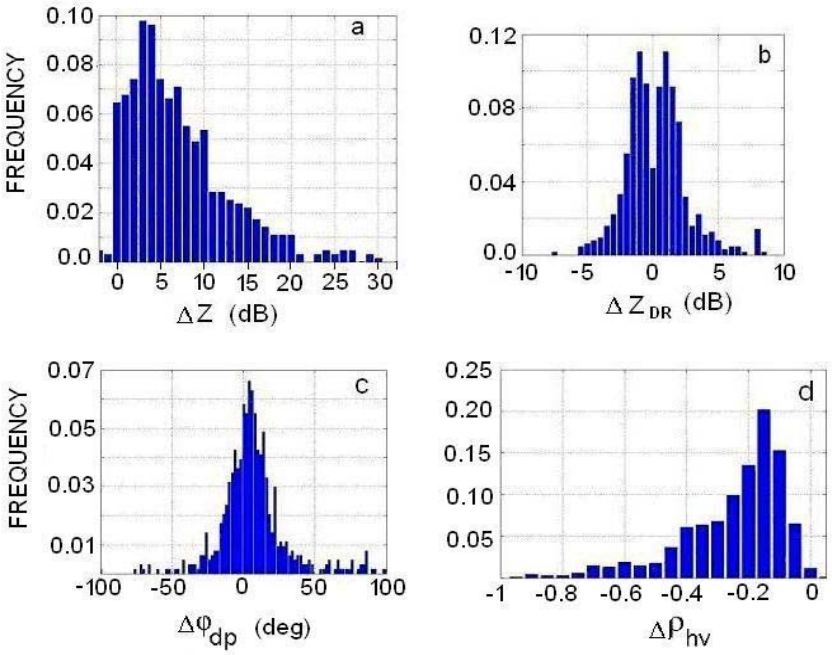

Fig. 3. Distributions of the deviations of (a) reflectivity, (b) differential reflectivity, (c) differential phase, and (d) copolar correlation coefficients from lightning.

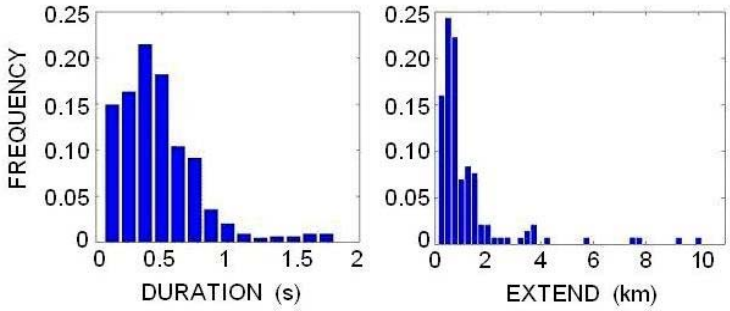

Fig. 4. Distributions of the (left) durations and (right) horizontal extent of lightning echoes.

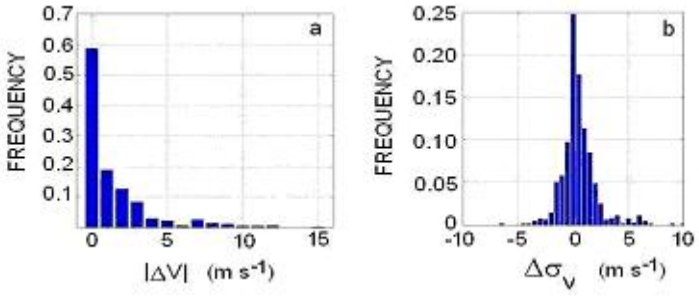

Fig. 5. Distributions of the deviations of (a) Doppler velocities and (b) spectrum widths in lightning echoes.

The criteria listed above helps isolate the lightning detection from natural fluctuations of the estimates that might occur in the absence of lightning. The probability that the deviations of estimates satisfy the criteria for hydrometeors is the false alarm rate, which should be sufficiently small; we require the rate to be less than 1%. It can be shown that probability of Z and Z_{DR} deviating by more than 3 and 1 dB simultaneously is 0.1% for SNR = 20 dB and 0.5% for SNR = 10 dB (ρ_{hv} = 0.95, σ_v = 1 m s^{-1}, M = 128). We therefore conclude that a SNR threshold of 10 dB can be used, which is substantially lower than 30 dB utilized in CCBM. This allows us to detect more lightning.

b) Deviations of polarimetric variables at lightning

The KOUN data analyzed in this study was collected on 19 days from 2002 to 2006. Overall, 223 lightning events on these 19 days were identified using the criteria listed above. Because the lightning event may contain several contiguous range gates, the total number of range gates with lightning echoes was determined to be 771. In this section, we present statistics of the deviations in the polarimetric variables caused by lightning in these radar resolution volumes.

Distributions of the deviations of polarimetric variables are presented in Fig. 3. 70% of deviations of reflectivity exceed 3 dB, with a maximum at 3-4 dB. In almost 30% of cases, the increase of reflectivity exceeded 10 dB. The distribution of Z_{DR} deviations is nearly symmetrical with maxima at ±1 dB and the width of absolute deviations of 1.5 dB. In 65% of cases, the deviations exceeded 1 dB. In CCBM, a similar distribution was found for Florida but with a small bias of -0.2 dB and slightly smaller width of 1.2 dB. The two-peak distribution of Z_{DR} is an intriguing feature. Analyzing power distributions in lightning echoes, Williams et al. (1989) came to the conclusion that the echoes are formed by many reflectors in the radar volume. Comparing data for S- and X-bands, they concluded that plasma in lightning channels is overdense (see also Caylor et al., 1993), so that scattering of electromagnetic waves can be considered as reflections from many metal wires. If lightning channel elements are distributed uniformly in the radar volume then a one-peak distribution of ΔZ_{DR} should be observed, which is not the case. A two-peak distribution could result from the fact that lightning has two major types: intra-cloud and cloud-to-ground discharges. With the first type, the lightning branches have a preferred horizontal alignment that results in positive Z_{DR} whereas, with the second type, the branches are oriented preferably vertically and produce negative Z_{DR}. Thus the total distribution would be expected to have a two-peak form.

Deviations of the differential phase reported in CCBM are smaller than for our data (Fig. 3c). A small 0.7^o positive bias was reported by CCBM; in our data, the mean is 8^o. Our distribution is also wider (SD = 24^o) than in CCBM (SD = 9.5^o). The φ_{dp} bias cannot be explained with the theory of scattering by thin wires. According to Van Fleck et al. (1947), the differential phase for a thin cylindrical conductor is zero.

The distribution of the copolar correlation coefficients in CCBM has a mean of 0.8 and a width of 0.086. Our data has nearly the same mean, i.e., 0.75, but a wider distribution, i.e., 0.17 (Fig. 3d). No ρ_{hv} drops of more than 0.45 were reported in CCBM. On the other hand, we have registered drops down to 0.05, which is almost the full possible magnitude. Our data also shows a correlation between deviations in Z and ρ_{hv}. That is, strong Z deviations are typically associated with large drops in ρ_{hv}.

Distributions of the duration and extent of lightning echoes are shown in Fig. 4. The durations are for a single range gate. The dwell time for data collection on the WSR-88D network is about 50 ms. From the left panel of Fig. 4, it can be seen that it is possible for several dwell intervals to be affected by lightning echoes. The right panel of Fig. 4, shows that 70% of lightning echoes extend less than 1 km, i.e., four or fewer 250-m range radar gates are affected by lightning. A significant percentage, however, have extents that reach 10 km.

Statistics of lightning radar echo parameters show that the hail detection algorithm experience the strongest impact from lightning. The longevity of a lightning echo can reach several radar dwell times and the radial extent can be several kilometers. These comprise an area comparable to hail cores. Because correlation coefficients drop significantly at lightning, those echoes can be easily misclassified as hail. We have not yet found a radar moment that allows distinguishing hail from lightning.

c) Deviations of the Doppler moments. Doppler spectra

Lightning can change Doppler spectra of scattered signals (Zrnic et al. 1982, Mazur et al. 1987). Therefore, the spectral moments can be used to recognize lightning. Lightning echoes are reflections from ionized air. At stages with electric currents, the lightning channels can be moved by

cloud electric fields, the magnetic field of the Earth, and the buoyancy force. Mazur et al. (1987) have measured accelerations of lightning echoes up to 120 m s^{-2}. Lightning channels at cooling stages can be considered as passive inclusions and thus should have spectral parameters close to the ones for the hydrometeors.

Fig. 5 presents distributions of deviations of Doppler velocities and spectrum widths in lightning echoes. The distribution of deviations of the Doppler velocities is symmetrical around zero and the histograms of the absolute deviations are shown in Fig. 5a. About 80% of the flashes have velocity deviations of less than 1 m s^{-1}. For flashes with stronger reflectivity deviations ($\Delta Z > 10$ dB), however, 56% of deviations exceeded 1 m s^{-1}. That is, stronger power deviations have greater velocity variations.

The distribution of the spectrum widths is nearly symmetrical (Fig. 5b) with a mean of 0.9 m s^{-1} and a width of 1.6 m s^{-1}. The positive bias indicates that, in the mean, lightning increases the spectrum widths, but that this increase is rather small. For stronger power deviations ($\Delta Z > 10$ dB), 65% of spectrum width deviations are greater than 1 m s^{-1}. There is a correlation between the power and width deviations.

The Doppler spectra of strong lightning echoes ($\Delta Z > 15$ dB) are quite broad. An example is shown in Fig. 6. Panels 1 and 4 correspond to times before and after the event while panels 2 and 3 present the spectra at the time of the lightning flash. For ρ_{hv} greater than 0.95, the strongest parts of the Doppler spectra at horizontal and vertical polarizations repeat each other in detail (panels 1 and 4). At the time of the lightning flash, ρ_{hv} decreases and the spectra differ. The radar parameters for the panels are shown in table 2. It is seen from the table that the power increases by approximately 25 to 27 dB at lightning and that all radar variables experience significant changes.

Table 2. Radar variables for four spectra shown in Fig. 6.

Panel	Z, dBZ	V, m s^{-1}	σ_v, m s^{-1}	Z_{DR}, dB	φ_{dp}, deg	ρ_{hv}
1	29.8	4.4	4.6	0.3	43	0.995
2	55.5	1.0	6.7	-2.2	29	0.823
3	57.1	-1.9	6.8	-1.0	46	0.705
4	29.4	4.0	4.7	0.5	45	0.980

We have not noticed any significant changes in reflectivity in radar resolution volumes after lightning flashes. Rather, reflectivity appears to return to the value measured before the flash. This means that strong acoustic waves accompanying the lightning flash do not noticeably affect hydrometeors in the radar resolution volume. Therefore, we can assume that the Doppler spectrum at lightning is a sum of the hydrometeor's spectrum and the one from the lightning flash itself. To obtain the latter, we can subtract the hydrometeor's spectrum from the measured one. To obtain the hydrometeor's spectrum in Fig. 6, we averaged four spectra: the two spectra measured before the lightning, i.e., the one shown in panel 1 and the previous one (not shown), and the two spectra measured after the lightning, i.e., the one shown in panel 4 and the next one (not shown). Because the hydrometeor's spectral powers are 20-25 dB smaller than the total spectra, panels 2 and 3 can be considered to be the lightning spectra.

d) Small number of samples. Possible PAR implication

Most of the KOUN's lightning data have been collected with a sufficiently large number of samples, i.e., $M = 128$, to produce good estimates of hydrometeor parameters. Unfortunately, such a large number of samples also smooths the estimates of transient lightning returns. We therefore processed time series data to analyze the M-dependences of lightning echo parameters. Using 128 samples we detected a lightning event on criteria described earlier and then analyzed the lightning parameters estimated with smaller number of samples.

Fig. 7 presents an example of the radar polarimetric parameters calculated with $M = 128$, 64, 32, 16, and 8. In the ΔZ panel (top left), it can be seen that $M = 32$, 16, and 8 all exhibit a two-peak pattern, whereas the second hump is not seen at $M = 64$ and 128. The ΔZ peaks correspond to the two minima in ρ_{hv} for $M = 32$, 16 and 8. KOUN's data show a significant correlation between the raise of Z and the drops of ρ_{hv} at the time of the lightning flash. An increase in M makes ρ_{hv} deviations smaller with the difference of ρ_{hv} at M=128 being more than two times that for M= 8. ΔZ_{DR} and $\Delta\varphi_{dp}$ for $M = 8$, 16, and 32 experience rather random and deep oscillations.

Phased array weather radars (PAR) can scan clouds fast. A short update time is achieved with a smaller number of samples, among other options (Heinselman et al., 2007). The described results on time-series analysis show that lightning can be detected with a PAR. It is possible even to track lightning with a PAR because such a radar steers the beam electronically in contrast to conventional mechanical antennas.

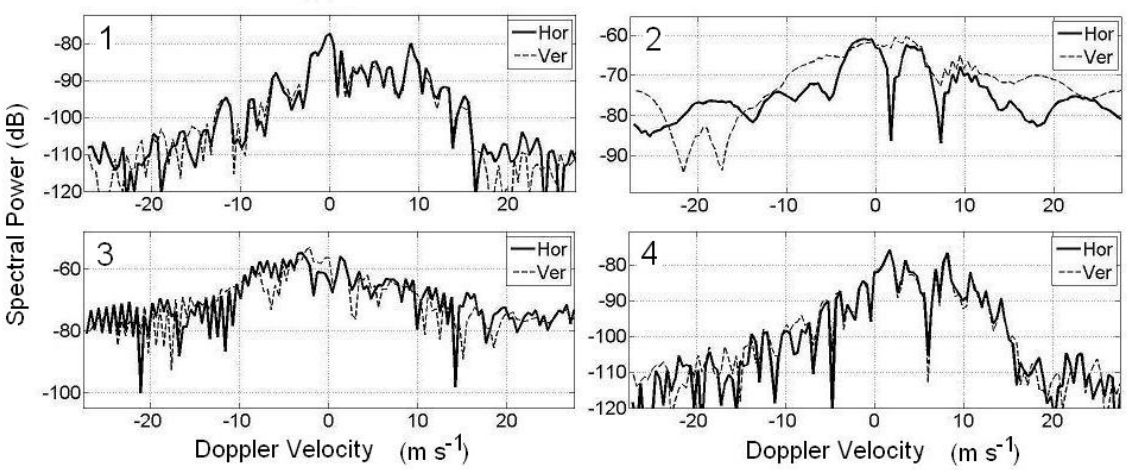

Fig. 6. Consecutive Doppler spectra at (the solid lines) horizontal and (the dash lines) vertical polarizations before (panel 1), during (panels 2 and 3), and after (panel 4) lightning. The spectral powers are in the inner processor units. 17 June, 2006 at 0452:16, azimuth is 280°, elevation is 8.8°, the height of the radar volume is 10.2 km, Von Hann spectral window, M = 128, PRF = 1013 Hz.

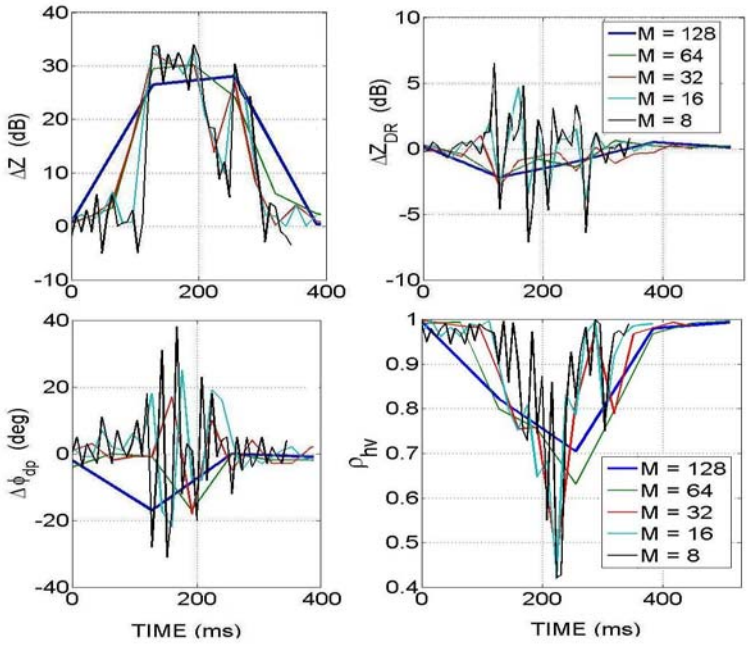

Fig. 7. Radar variables at lightning calculated with 8, 16, 32, 64, and 128 samples. 13 June, 2005 at 2203, azimuth is 191°.

2. Parameters of lightning echoes in LDR mode

The SHV configuration is the main polarimetric mode for the WSR-88Ds. Research WSR-88D KOUN can operate in another polarimetric mode during which all of the power is injected into horizontal plane and radar returns are received at both polarizations. In this mode, six radar variables are calculated in each range gate: reflectivity, the Doppler velocity, spectrum width (these are calculated in the H-channel), linear depolarization ratio, L_{DR}, the differential phase, and cross-polar correlation coefficient, ρ_{xh}, where the second subscript denotes horizontal incidence and the first one stands for orthogonal receive polarization which is vertical for KOUN.

The left panel in Fig. 8 presents L_{DR}. The melting layer is clearly seen at heights near 4 km. The layer is not as pronounced beyond 80 km in an area of strong convection. Strong depolarization is also seen at heights from 7 to 10 km in the far cell, which is an area of strong electric fields with aligned crystals. This conclusion is supported by the field of the cross-polar coefficient (Fig. 8 right). The strongest L_{DR} is seen at distances of 110 – 130 km and just above the melting layer at heights of 4 to 6 km. L_{DR} in these spots, which are believed to be echoes from lightning, reach -10 dB.

a) Radar data processing

Like in the SHV mode, data collected using LDR mode have been recorded with the antenna either stationary or moving very slowly. For a moving antenna, vertical radar cross sections with vertical scanning rates less than 0.2 deg s^{-1} have been analyzed. An example of range profiles of the polarimetric variables during lightning flashes is shown in Fig. 9, which presents four consecutive profiles obtained with 256 samples at a pulse repetition frequency of 1013 Hz. During the event, the antenna was raised by only 0.22^o. The lightning echo is seen as strong perturbations of both Z and L_{DR} at distances of 36 to 40 km in the two inner profiles. The first and last profiles are close to each other and represent the profiles before and after lightning. Lightning echoes have been identified by inspecting consecutive radials. A group of radials with close first and last ones in Z and L_{DR}, and significant deviations of the variables in between, has been identified as a lightning echo. The deviations are considered significant if at least one profile in the group had a deviation in Z grater than 3 dB and a deviation in L_{DR} grater than 5 dB at least in one range gate. SNR in the vertical channel was larger than 10 dB before lightning (Table 3).

Table 3. Criteria of lightning echo recognition in LDR mode

Parameter	Value
SNR, dB	10
Z deviation, dB	3
L_{DR} absolute deviation, dB	5

In LDR mode, the correlation coefficients of weather echoes without lightning are typically low, reaching 0.9 in areas of strongly aligned crystals. At low ρ_{xh}, fields of ρ_{xh} and φ_{dp} are noisy which makes them difficult to use forlightning detection, which is in contrast to φ_{dp} and ρ_{hv} in SHV mode. L_{DR} deviations, however, delineate lightning echoes well. The probability that the deviations of reflectivity of weather echo (not lightning) exceeds 3 dB is 0.2% and the probability that the L_{DR} deviation exceeds 5 dB is less than 0.06% (M=128, σ_v = 2 m s^{-1}, SNR_v = 10 dB), and probability of ΔZ>3dB &|ΔLDR|>5dB is less than 10^{-4}%. So that the criteria of lightning echo recognition listed in Table 3 have an extremely low false alarm rate.

b) Deviations of radar variables at lightning

The data analyzed contains 9 days in 2002 to 2006 with 149 lightning events. Distributions of L_{DR}, ρ_{xh}, and φ_{dp} deviations at lightning are presented in Fig. 10. 93% of deviations of L_{DR} exceed 5 dB, with a maximum at 13-14 dB, and the mean of 14.5 dB. The standard deviation of the distribution is 5.1 dB. The distribution of $\Delta\rho_{xh}$ has a mean of 0.13 with a standard deviation of 0.18. The distribution of $\Delta\varphi_{dp}$ is broad with a mean of 12^o and a standard deviation of 46^o. In LDR mode, ρ_{xh} and φ_{dp} experience strong fluctuations in precipitation so these parameters are not appropriate for lightning echo recognition. L_{DR} experiences strong deviations at lightning thus the deviations of Z and *LDR* can be utilized in the recognition.

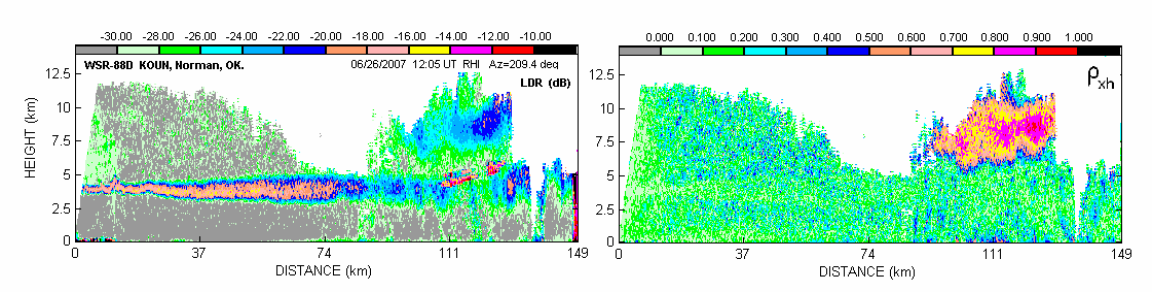

Fig. 8. Vertical cross section of L_{DR} (left panel) and ρ_{xh} (right panel) collected on 26 June, 2007 at 1205 in Az = 209.4°.

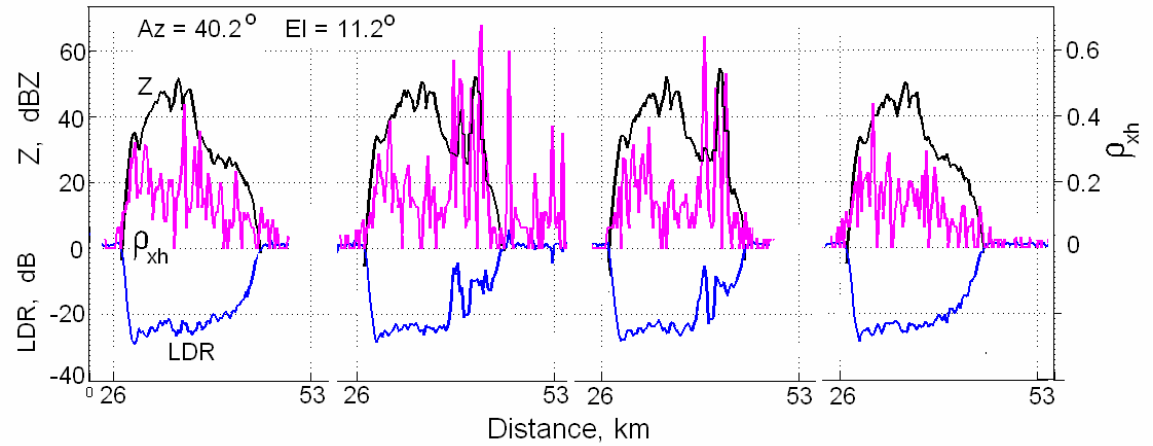

Fig. 9. Consecutive range profiles of Z, L_{DR}, and ρ_{xh} on 18 March, 2003 at 0121:050. M =256, PRF = 1013 Hz.

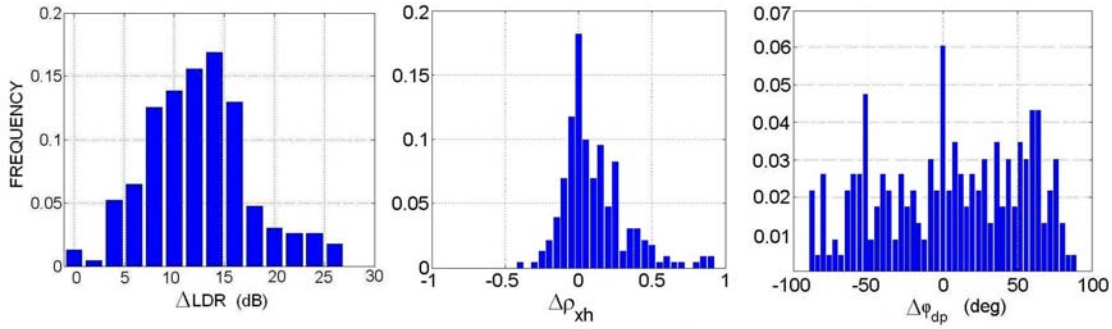

Fig. 10. Distributions of the deviation of (left) L_{DR}, (center) ρ_{xh} , and (right) φ_{dp} in lightning echoes. WSR-88D KOUN.

The mean ΔL_{DR} at strong lightning ($\Delta Z >$ 15 dB) obtained with our data is -12 dB. Frequently, a radar echo of lightning, assuming that plasma in lightning is overdense, is modeled as an echo from randomly distributed wires (e.g., Williams et al. (1989) and CCBM) . The copolar and cross-polar powers of radiation scattered by wires can be written as (Van Fleck et al., 1947): $P_h = A(\theta) \cos^4\varphi$, $P_v = A(\theta) \cos^2\varphi \sin^2\varphi$, where θ is the angle between the direction of wave propagation and the wire, $A(\theta)$ is a function of θ, the diameter of the wire, its length, and the wavelength, φ is the angle between incident electric field and a plane formed by the direction of incidence and the wire. For random spatial distribution, $<L_{DR}> = <\cos^2\varphi \sin^2\varphi>/<\cos^4\varphi> = 0.33$ that equals -4.7 dB (angular brackets stand for ensemble averaging). The latter value is in contrast with the experimental result. Considering circular polarization data obtained at L-band, Mazur and Walker (1982) came to the conclusion that lightning channels are primarily oriented horizontally. Our data collected in SHV mode (section 2) do not support such an assumption. Further discussion on discrepancies between the experimental and theoretical results obtained under certain assumptions is beyond the scope of this paper.

c) Doppler spectra

An example of the Doppler spectra at two polarizations is shown in Fig. 11. Panels 1 and 6 correspond to the times before and after the lightning event. Corresponding radar parameters are shown in Table 4. From the table, it can be seen that the power at horizontal polarization changes by about 5 dB at the time of the lightning flash, whereas at cross-polarization, it changes by more than 20 dB. ρ_{xh} changes insignificantly during the event, whereas φ_{dp} experiences large alternations. The Doppler velocities and spectrum widths differ significantly at two polarizations: frequently, the widths at the cross-channel are wider than the ones at the co-channel. Like for the SHV mode, the main spectral lobes remain at about same frequencies during lightning. It should be noted a big rise in the spectral "skirts" in both channels during lightning: the increase can reach 25 – 30 dB. This feature can be used for lightning recognition.

5. Conclusions

Lightning causes two types of "outlier" radar echoes in clouds and precipitation: 1) reflections from lightning channels (e.g., Fig. 1b), and 2) radials contaminated with strong noise caused by intercepted lightning radiation (e.g., Fig. 1c). In SHV polarimetric mode, the second type of "outlier" can be eliminated or significantly reduced with the 1-lag estimators of polarimetric parameters, which are immune to noise.

Experimental data on radar lightning echo statistics at S-band are presented for central Oklahoma. The distribution of ΔZ_{DR} is symmetrical and has two strong peaks (Fig. 3b). A similar distribution was obtained by Caylor et al. (1993) in Florida, but with a more shallow "saddle". Such distributions might be caused by two types of lightning: 1) cloud-to-ground discharges that are preferentially oriented in vertical channels, which could result in the negative peak of ΔZ_{DR}, and 2) intra-cloud discharges that are preferentially oriented in horizontal channels, which could cause the positive peak of ΔZ_{DR}.

In lightning echoes, polarimetric radar parameters can experience significant alternations (Fig. 2). The hail detection algorithm, which is highly dependent on a lowering of the copolar correlation coefficient, can easily misclassify lightning echoes as hail. The longevity of lightning echo can reach several radar dwell times and the radial extent can be up to several kilometers, which comprises an area comparable to that of hail cores.

Deviations of the Doppler velocities and spectrum widths during lightning flashes are not large with 80% of the velocity deviations and 70% of the spectrum width deviations being less than 1 m s^{-1}. No significant shifts in the main parts of the Doppler spectra have been noticed in the H and V channels at lightning although the spectral lines can differ. This can be interpreted by considering the elements of lightning echoes as passive inclusions driven by the wind. The data show a significant (up to 30 dB) rise in spectral "skirts" at lightning. This feature can be used for lightning recognition.

Using a small number of samples, i.e., M = 8 to 20, allows for the detection of "fine" time structure of lightning echoes. Deviations of reflectivity and ρ_{hv} can be deeper for small number of samples than with regular M of about 50 for the WSR-88Ds. A small number of samples can be implemented with polarimetric phased array radars to map and track lightning echoes.

In LDR mode, lightning echoes can be recognized using deviations of reflectivity and the linear depolarization ratio, L_{DR}. The mean increase in L_{DR} during a lightning discharge is 13-14 dB, reaching 27 dB in some cases. The cross-polar correlation coefficient and differential phase experience strong fluctuations in hydrometeors and lightning and the data show their low potentials in lightning recognition. Frequently, a raise in spectral "skirts" up to 30 dB is observed. This also can be used in lightning recognition.

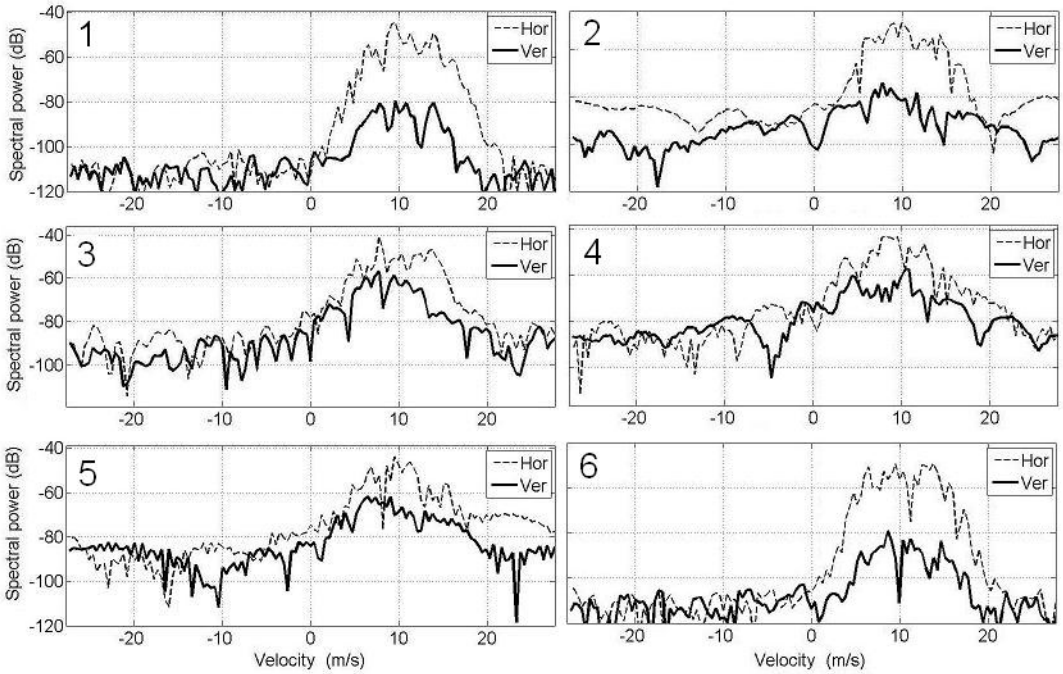

Fig. 11. Six consecutive 128-sample spectra in the co and cross-polar channels
on 25 June, 2006 at 2316:44, R=78.3 km, H= 6.7 km, azimuth is 315°, Von Hann spectral window.

Table 4. Radar parameters for six panels shown in Fig. 11.

Panel	Z, dB	LDR, dB	ρ_{xh}	φ_{dp}, deg	V_h, m s^{-1}	V_h, m s^{-1}	$\sigma_{v(h)}$, m s^{-1}	$\sigma_{v(v)}$, m s^{-1}
1	53.0	-32.0	0.26	202	10.3	10.1	2.1	3.4
2	53.5	-16.8	0.23	159	9.7	7.5	2.6	6.2
3	56.3	-11.7	0.31	43	10.0	8.4	2.9	2.7
4	58.1	-15.2	0.30	296	9.0	8.1	2.4	4.9
5	55.2	-15.1	0.25	74	9.8	8.0	2.5	4.9
6	52.3	-31.1	0.23	117	10.9	9.0	2.8	3.6

References

Atlas, D., 1958: Radar lightning echoes and atmospherics in vertical cross section. Recent Advances in Atmospheric Electricity. L.G. Smith, Ed., Pergamon Press.

Bluestein, H.B., S. J. Frasier, R. Bluth, I.PopStefanija, R. L. Tanamachi, M. M. French, J. C. Snyder, J. B. Houser, P. S. Tsai, M. Ohene, and C. Baldi. 2007: Preliminary results from the fielding of a disparate triad of mobile Doppler radars to study severe convective storms and tornadoes. 33rd Weather radar conference, Cairns, Australia. 13A.2.

Bringi, V. N., and V. Chandrasekar, 2001: *Polarimetric Doppler Weather Radar. Principles and Applications.* Cambridge University Press. 636 pp.

Cate, G.S, and R.W. Hall, 2005: MCNA NEXRAD Product Improvement – Current Status of WSR-88D Open Radar Data Acquisition (ORDA) Program and plans for the Future. *21st Internat. Conf. on Interactive Information Proc. Sys. for Meteorol., Ocean., and Hydr.*, (*IIPS*) AMS, San Diego, CA, 5.2.

Caylor I.J., V. Chandrasekar, V.N. Bringi, and S.S. Minger, 1993: Multiparameter radar observations of lightning. *Prepr. 26th Weather Radar Conf.,* AMS, Boston, 306-308.

Caylor I.J., and V. Chandrasekar, 1996: Time-varying ice crystal orientation in thunderstorms observed with multiparameter radar. *IEEE Trans.* **GRS-34**, 847-858.

Doviak, R. J. and D. S. Zrnic, 1993: *Doppler radar and weather observations*, 2nd ed., Academic Press, 562 pp.

Doviak, R.J., V. Bringi, A. Ryzhkov, A. Zahrai, and D. Zrnic, 2000: Considerations for polarimetric upgrades to operational WSR-88D radars. *J. Atmos. Oceanic Technol.* **17**, 257 – 278.

Forsyth, D. E., J. F. Kimpel, D. S. Zrnic, R. Ferek, J. F. Heimmer, T. J. McNellis, J. E. Crain, A. M. Shapiro, R. J. Vogt, and W. Benner, 2005: The National Weather Radar Testbed (Phased-Array). *32th Weather Radar Conf.,* AMS, Albuquerque, N.M., 12R3.

Heinselman, P.L., K.L. Manross, and D.L. Priegnitz, 2007: Comparison of storm evolution characteristics: The NWRT and WSR-88D. 23rd International Conference on Interactive Information Processing Systems for Meteorology, Oceanography, and Hydrology, AMS, San Antonio, TX, 7.5.

Hendry A., and G. C. McCormick, 1976: Radar observation of the alignment of precipitation particles by electrostatic fields in thunderstorms. *J. Geophys. Res.,* **81**, 5353-5357.

Istok, M.J., M. A. Fresch, S. D. Smith, Z. Jing, R. Murnan, A. V. Ryzhkov, J. Krause, M. H. Jain, J. T. Ferree, P. T. Schlatter, B. Klein, D. J. Stein, G. S. Cate, and R. E. Saffle. 2009: WSR-88D Dual Polarization Initial Operational Capabilities. 25th Conf. IIPS, Phoenix, Az. 15.5.

Jenkins, G.M., and D.G. Watts, 1968: *Spectral analysis and its applications*. Holden-Day, Inc., San-Francisco, 525 pp.

Krehbiel, P.R., W. Rison, S. McCrary, T. Blackman, and M. Brook, 1991: Dual-polarization radar observations of lightning echoes and precipitation alignment at 3-cm wavelength. *Prepr. 25th Weather Radar Conf.,* AMS, Boston, 901-904.

Krehbiel, P.R., T. Chen, S. McCrary, W. Rison, , G. Gray, T. Blackman, and M. Brook, 1992: Dual polarization radar signatures of the potential for lightning in electrified storms. *9th Int. Conf. Atmos. Elect.,* St. Petersburg, Russia, 166-169.

Liu, H., and V. Chandrasekar, 2000: Classification of hydrometeors based on polarimetric radar measurements: development of fuzzy logic and neuron-fuzzy systems, and in situ verification. *J. Oceanic Atmos. Technol.*, **17**, 140-164.

Mazur, V., and G. B. Walker, 1982: The effects of polarization on radar detection of lightning. *Geophys. Res. Letters*, **9**, 1231-1234.

Mazur, V., D. S. Zrnic, and W. D. Rust, 1985: Lightning channel properties determined with vertically pointing Doppler radar. *J. Geophys. Res.,* **90**, 6165-6174.

Mazur, V., D. S. Zrnic, and W. D. Rust, 1987: Transient changes in Doppler spectra of precipitation associated with lightning. *J. Geophys. Res.,* **92**, 6699-6704.

Melnikov, V. M., and D. S. Zrnic, 2007: Autocorellation and cross-correlation estimators of polarimetric variables. *J. Atmos. Oceanic Technol*., **24,** 1337-1350.

Metcalf, J.I., 1995: Radar observations of changing orientations of hydrometeors in thunderstorms. *J. Applied Meteorol.,* **34**, 757-772.

Schuur, T., A. Ryzhkov, and P. Heinselman, 2003: Observations and classification of echoes with the polarimetric WSR-88D radar. NOAA/NSSL Report. 45 pp. (Avialable online at www.cimms.ou.edu/~schuur/jpole/WSR-88D_reports.html).

Van Fleck, J. H., F. Bloch, and M. Hamermesh, 1947: Theory of radar reflection from wires or thin metallic strips. *J. Applied Phys*., **18**, 274–294.

Williams, E. R., S. G. Geotis, and A.B. Bhattacharya. 1989: A radar study of the plasma and geometry of lightning. *J. Atmos. Sci.,* **46**, 1173-1185.

Zrnic, D. S., W. D. Rust, and W.L. Taylor, 1982: Doppler radar echoes of lightning and precipitation at vertical incidence. *J. Geophys. Res.,* **87**, 7179-7191.

Zrnic, D.S., and A. V. Ryzhkov, 1999: Polarimetry for weather surveillance radar. *Bull. Amer. Meteorol. Soc*., **80**, 389-406.

Zrnic, D.S., A. V. Ryzhkov, J. Straka, Y. Liu, and J. Vivekanandan,1999: Testing a procedure for automatic classification of hydrometeor types. *J. Oceanic Atmos. Technol.*, **18**, 892-913.